Tranexamic acid-loaded mesoporous silica microspheres as a hemostatic material

Materials Today Communications 34 (2023) 105198

Contents lists available at ScienceDirect

Materials Today Communications

journal homepage: www.elsevier.com/locate/mtcomm

Tranexamic acid-loaded mesoporous silica microspheres as a hemostatic material

Sara Saber Younes Mohamed [a], Alberto Gambino [a], Mauro Banchero [a], Silvia Ronchetti [a], Luigi Manna [a], Roberta Cavalli [b], Barbara Onida [a,*]

[a] Department of Applied Science and Technology, Politecnico di Torino, Corso Duca degli Abruzzi 24, 10129 Torino, Italy
[b] University of Turin, Department of Drug Science and Technology, via Pietro Giuria 9, 10125 Turin, Italy

ARTICLE INFO

Keywords:
Hemostasis
Mesoporous silica
Tranexamic acid
Incipient wetness impregnation
Release

ABSTRACT

Bleeding management is considered essential for saving life both in the military and civilian field. There is still a need to develop topical hemostats that can stop bleeding and be used easily in the trauma sites. The aim of this work is to develop a hemostat based on mesoporous silica particles with large pores for bleeding control. Mesoporous silica microspheres (MSM) with particle size of 1.5 − 5 μm and pores diameter of 25 nm have been successfully synthesized and, for the first time, loaded with tranexamic acid (TXA) with a content of 4.7%w/w. The hemostatic activity of both the pure material and TXA-loaded material (TXA@MSM) was investigated. It was found that the blood clotting time was significantly shortened by both systems with respect to control. A hemolysis assay was performed to evaluate the hemolytic activity of MSM, and the result indicated that the material was blood compatible. A preliminary TXA in vitro release test was performed, showing the complete release of TXA from the carrier within one hour. Considering the above results, TXA@MSM can be considered a promising material for the development of new hemostats.

1. Introduction

The uncontrolled bleeding that may follow major traumas remains one of the most common causes of potentially preventable death among injured patients [1]. The World Health Organization (WHO) estimated that in 2000 injuries accounted for 9% of global mortality and 12% of global burden diseases [2]. In 2015, the American National Institute of Trauma estimated that hemorrhages were responsible for over 35% of pre-hospital deaths and about 40% of deaths within the first 24 h after injury in civilian hospitals [3]. In addition, in case of victims' survival, the initial large blood loss could impair wound healing, increase the risk of infections and organ failure so resulting in late morbidity and mortality risk and high economic cost of care [4]. Therefore, an early and rapid management of bleeding is considered critical for life saving. A large variety of products, which include active and non-active hemostats, have been developed and suggested to be used in the management of bleeding. Active hemostatic agents are a class of products that contain one or more active proteins such as fibrin, thrombin, and collagen, but are very difficult to use outside hospitals since they require special storage conditions [5]. Moreover, active hemostats could induce allergic reactions due to the presence of animal- or human-derived proteins [6]. To overcome these limitations and facilitate the achievement of hemostasis in emergency (for instance in the battlefield or in trauma sites), topically applied non-active materials, which do not contain proteins, have been developed and used to control bleeding [7]. Hemostats based on inorganic materials, which include zeolites (i.e., QuikClot™), have been recommended in the management of massive bleeding by the Committee on Tactical Combat Casualty Care (CoTCCC) since they are animal-protein or human-protein free and very efficient [6]. However, patients treated with QuikClot agents experienced adverse effects such as thermal tissue injuries and abnormal foreign-body reactions due to the exothermic process of action and poor biodegradability of these materials [8]. Therefore, there is still a need to develop alternative effective hemostatic materials able to control hemorrhages and reduce collateral effects.

Recently, mesoporous silica-based materials (MS) have attracted much attention as hemostats due to their biocompatibility, biodegradability and unique physiochemical properties including high surface area, high pore volume and large pore size [9–17]. As zeolites, MS have shown great potential in promoting the clotting process and achieving

* Corresponding author.
E-mail address: barbara.onida@polito.it (B. Onida).

https://doi.org/10.1016/j.mtcomm.2022.105198
Received 5 April 2022; Received in revised form 6 December 2022; Accepted 16 December 2022
Available online 19 December 2022

hemostasis without causing any adverse side effect. Owing to their high porosity and large pore size, MS are able to achieve hemostasis by absorbing a large amount of water from the blood and concentrating the clotting factors and platelets at the bleeding site: this mechanism of action allows them to be classified as factor concentrators. Moreover, the presence of a high concentration of polar silanols and negative net charges at the surface of MS is beneficial to blood coagulation as it can activate factor XII and other clotting proteins, which is known as the procoagulant effect [6,14,18]. Various studies have investigated the effect of specific surface area and pore size on the hemostatic ability as they are considered important factors in improving the adsorption capacity of these materials. The effect of specific surface area on the hemostatic efficiency of mesoporous silica xerogels was investigated by Wu et al. [11] whose results indicated that the prothrombin time (PT, i.e. the time to activate the extrinsic pathway) and the activated partial thromboplastin time (APTT, i.e. the time to activate the intrinsic pathway) were shortened by the presence of a mesoporous silica xerogel with respect to non-mesoporous silica xerogel and control. The authors ascribed the clotting ability of the mesoporous silica xerogel to its high surface area, which improved the water absorption capability of the material and resulted in higher concentration of the blood components and the consequent reduction of clotting time. Chen et al. [14] investigated the hemostatic performance of MS nanoparticles with different pore and particle sizes. The results of the clotting blood tests showed that the hemostatic efficiency of the nanoparticles was influenced by the pore size rather than the particle size and it was maximum for those nanoparticles with a pore size larger than 10 nm.

Given the above premises, the aim of this work is the development of a topical hemostat based on large pore MS to be used in the management of massive bleeding in emergency situations. To further enhance the hemostatic performance, MS was loaded with tranexamic acid (TXA). TXA, trans-4-(aminomethyl) cyclohexanecarboxylic acid, is a synthetic antifibrinolytic drug widely used to manage the excessive blood loss that results from trauma, surgery or bleeding disorders. It is a derivative of lysine and it inhibits the breakdown of fibrin clot by reversibly binding to the lysine-binding sites on plasminogen molecules, thereby stabilizing the clot and preventing the excessive bleeding caused by hyperfibrinolysis [19]. However, TXA presents a low bioavailability and causes several adverse effects, which include gastrointestinal disorders when administered orally, and hypotension when administered intravenously [20]. An effective alternative approach to improve the efficacy of TXA is to apply it topically [21] and use appropriate carriers to control its release [20,22]. To the best of the authors' knowledge, the combination of mesoporous silica with tranexamic acid has not been reported yet. To this purpose, mesoporous silica microspheres (MSM) with large pores have been synthesized and, for the first time, loaded with TXA to prepare a material that combines the intrinsic hemostatic properties of MS and the antifibrinolytic activity of TXA. The characterization of the MSM before and after the loading with TXA was performed using different techniques such as nitrogen sorption analysis, X-Ray Diffraction (XRD) and Fourier Transform Infrared spectroscopy (FT-IR). A blood clotting time test and a hemolysis assay were carried out on the materials to evaluate their hemostatic ability and blood compatibility, respectively. Finally, a preliminary in vitro release test was performed in an isotonic solution (NaCl 0.9% w/v) to determine the release ability of the carrier.

2. Materials and methods

2.1. Materials

Pluronic P123, tetraethyl orthosilicate (TEOS, 99.999% trace metals basis), hydrochloric acid (ACS reagent, 37%), potassium chloride (KCl, ≥99,0%), mesitylene (98%), tranexamic acid (pharmaceutical secondary standard) and sodium chloride were purchased from Sigma-Aldrich (St. Louis, MO, USA). Water (LC-MS grade) was provided by Merck (Billerica, MA, USA).

2.2. The synthesis of MSM

The procedure used for the preparation of MSM was adapted from that reported by Wang and coworkers [23]. It is a well-established method that allow a material with spherical morphology and large pores to be obtained, which is suitable for its final application. 4.0 g of Pluronic P123 and 6.1 g of KCl were dissolved in a mixture of 120 g of H_2O and 23.6 g of HCl (conc. 37%); then 3.0 g of TMB were added and the solution was stirred. After 2 h of stirring, 8.5 g of TEOS was added drop by drop and the mixture was stirred vigorously for 10 min. The final molar ratios of the reactants were 1 TEOS: 0.017 P123: 0.6 mesitylene: 2 KCl: 5.85 HCl: 165 H_2O. The mixture was maintained under static condition at 35 °C for 24 h, then it was transferred into a sealed PTFE bottle and kept at 100 °C for 24 h. The resulting white solid precipitate was filtered, washed with water, and dried at 60 °C in an oven for one night. The dried powder was calcined in air at 500 °C for 6 h in a muffle furnace to remove the template.

2.3. The loading of TXA

The loading of TXA was performed using water as a solvent through the incipient wetness impregnation technique. This method is simple, fast, economic and green since any organic solvent is employed, which make it suitable for a potential future industrial transfer. For the impregnation, 15 mg of TXA were dissolved in 0.36 ml of water, then the solution was added dropwise to 285 mg of MSM so that the nominal TXA content was about 5%w/w. The slurry was mixed vigorously using a spatula, and the sample was kept drying at room temperature overnight. The obtained material was designed as TXA@MSM.

To confirm that the TXA amount initially dissolved in the impregnating water solution had effectively been loaded on the carrier, TG analyses were performed using a SETARAM 92 instrument (Caluire, France) between 25 °C and 800 °C at the heating rate of 10 °C /min in air. The TXA content in the TXA@MSM sample was calculated from the weight loss between 200 °C and 800 °C by subtracting the weight loss measured in the same temperature range for the unimpregnated MSM (Fig. S1), and its amount resulted to be 4.7% w/w.

2.4. Instrumental Characterization

The morphology of the sample was characterized using a Field Emission Scanning Electron Microscope (FESEM Supra 40 instrument, Carl Zeiss, Oberkochen, Germany). Particle size distribution was calculated using the software "ImageJ." (Open source, https://imagej.net/) by analyzing 73 particles.

Nitrogen adsorption-desorption isotherms were obtained with a Micromeritics ASAP 2020 Plus Physisorption analyzer (Micromeritics, Norcross, GA, USA). Before the measurement, the unimpregnated sample was outgassed at 150 °C for 2 h, while the impregnated MSM was outgassed at 70 °C for 2 h. Specific surface area (SSA) was calculated using the Barret-Emmett-Teller (BET) method in the relative pressure range of 0.12–0.20. The total pore volume was determined at a relative pressure of about 0.99. The pore size distribution and the average pore size were obtained using the density functional theory (DFT) model.

Zeta potential measurements of MSM and TXA@MSM were performed using a 90 Plus Instrument (Brookhaven, New York City, NY, USA). The zeta potential values were determined by placing diluted samples in an electrophoretic cell, where an approximately 15-V/cm electric field was applied. All measurements were carried out in triplicate.

Wide angle X-Ray Diffraction (XRD) patterns were recorded on Panalytical X'Pert PRO (Malvern Panalytical, Almelo, The Neatherlands) using Cu-Kα radiation (40 kV, 40 mA). The data were collected from 5° to 60° (2θ) with a step size of 0.026° (2θ).

Fourier Transform Infrared (FT-IR) analysis was performed using an Equinox 55 spectrometer (Bruker, Billerica, MA, USA) on self-supported pellets, prepared by pressing the powder with a hydraulic press. All samples were outgassed in high vacuum (residual pressure equal to 0.1 Pa) at room temperature for 1 h. Spectra were obtained from 4000 cm^{-1} to 600 cm^{-1} with a resolution of 2 cm^{-1}.

2.5. In vitro blood Coagulation test

Blood clotting time (BCT) test is a simple method used to evaluate whole blood coagulation in vitro. The test was performed according to the procedure reported in literature [14,17]. Briefly, 3 mg of sample were put in an eppendorf tube and kept at 37 °C for 5 min. Then 250 μl of 3.2% sodium citrate rat blood was added to the sample, followed by vortexing for 10 s, and incubated at 37 °C for 3 min. After that, 25 μl of 0, 25 M calcium chloride ($CaCl_2$) aqueous solution was pipetted into the tube to activate blood coagulation. The tube was tilted every 15 s until the blood stopped to flow through the wall of the tube. The clotting time was used as the result of the BCT test.

2.6. Hemolysis assay

The hemolytic activity of the samples was evaluated on rat blood diluted with PBS pH 7.4 (1:10 v/v).

100 μl of the samples prepared in saline solution (NaCl 0.9% w/v) at two different concentration (1 mg/ml and 5 mg/ml) were incubated with 900 μl of diluted blood at 37 °C for 90 min, so that the final concentrations were 100 μg/ml and 500 μg/ml. After incubation, the samples were centrifuged at 2000 rpm for 10 min to separate the plasma. The amount of hemoglobin released in the supernatant due to hemolysis was measured spectrophotometrically at 543 nm (Du 730 spectrophotometer, Beckman).

The hemolytic activity was calculated with reference to complete hemolyzed samples (induced by the addition of Triton X-100 1% w/v to the blood, used as positive control) and negative control (NaCl 0.9% w/v).

$$\text{Hemolysis}(\%) = \frac{(Abssample - Absneg)}{(Abspos - Absneg)} x100$$

2.7. Preliminary in vitro release test of TXA

To assess the ability of TXA@MSM to release TXA, a dissolution test was carried out using an isotonic solution (NaCl 0.9% w/v) as the receiving medium. 10 mg of TXA@MSM were soaked in 10 ml of isotonic solution. After 60 min, the sample was recovered by filtration, dried upon complete evaporation of the solvent, and analyzed by FT-IR spectroscopy. The analysis was performed on a self-supporting pellet, prepared by pressing the powder with a hydraulic press. Before the measurement the sample was outgassed in high vacuum (residual pressure of 0.1 Pa) at room temperature for 1 h. Then, the achieved spectrum was compared with the spectrum of TXA@MSM, i.e., the sample before the dissolution test.

3. Results and discussion

3.1. MSM and TXA@MSM characterization

The characterization of the unimpregnated (MSM) and impregnated (TXA@MSM) material by means of FESEM, nitrogen sorption analysis, XRD and FT-IR spectroscopy is discussed hereafter.

Fig. 1 shows the FESEM images of MSM and the calculated particle size distribution. The material appears composed of spherical microparticles with a wide particle size distribution in the range of 1.5 − 5 μm.

a) b).

Nitrogen adsorption-desorption isotherms and pore size distribution of MSM and TXA@MSM are shown in Fig. 2. MSM presents a type IV isotherm (Fig. 2a, black lines), according to IUPAC classification, with a H5 hysteresis loop, which is characteristic of materials with both open and partially blocked mesopores [24]. The pore size distribution (Fig. 2b, black line) of MSM is unimodal and narrow with an average pore size of 25 nm. The values of SSA_{BET} and V_p are 342 m^2/g and 1.27 cm^3/g, respectively.

As far as the sample TXA@MSM is concerned, no significant change could be observed in the isotherm (Fig. 2a, red lines) neither in the pore size distribution (Fig. 2a, red line) when compared to MSM as such. The values of SSA_{BET} and pore volume of TXA@MSM are 325 m^2/g and 1.22 cm^3/g, respectively, i.e., almost negligibly lower than those measured for MSM before impregnation (Table 1). These results suggest that TXA molecules are well dispersed and homogeneously distributed on the surface of the mesopores. Indeed, due to the large pore size of MSM (25 nm), the limited amount of TXA molecules in TXA@MSM (0.092 mmol/m^2) and the small molecular size of TXA ($C_8H_{15}NO_2$, molecular weight 157.21, Scheme 1) it is not surprising that the presence of the guest TXA molecules on the surface of mesopores negligibly affects the porosity of the carrier.

Zeta potentials of MSM and TXA@MSM were determined to be -33.44 ± 2.91 mV and - 34.18 ± 2.26 mV, respectively. No significant change can be observed after TXA adsorption, suggesting that particles' external surface did not undergo significant modification upon TXA loading and that TXA molecules are mostly located inside the pores.

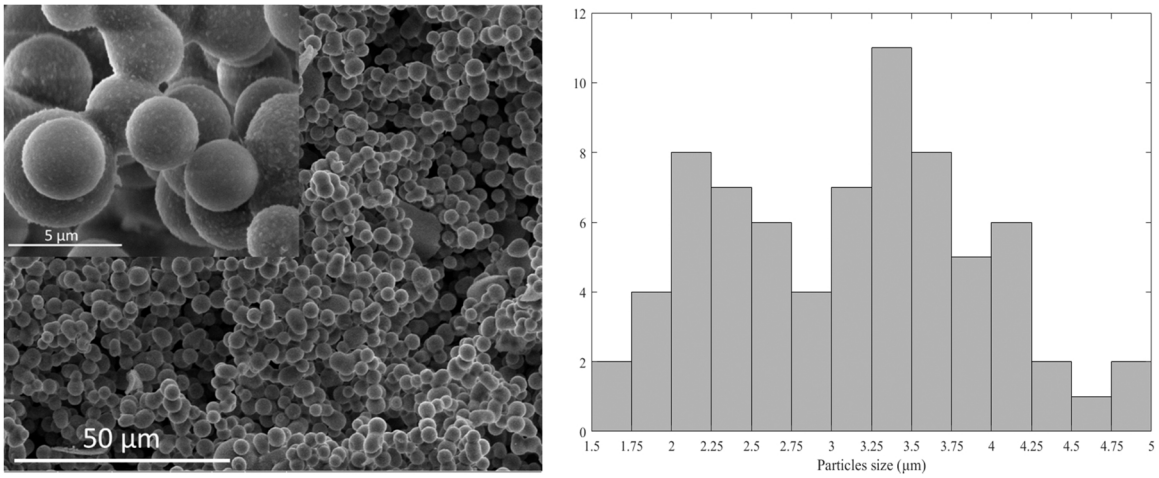

Fig. 1. (a) FESEM images (magnification: 1.00 K X and 10.00 K X in the inset) and (b) particle size distribution of MSM.

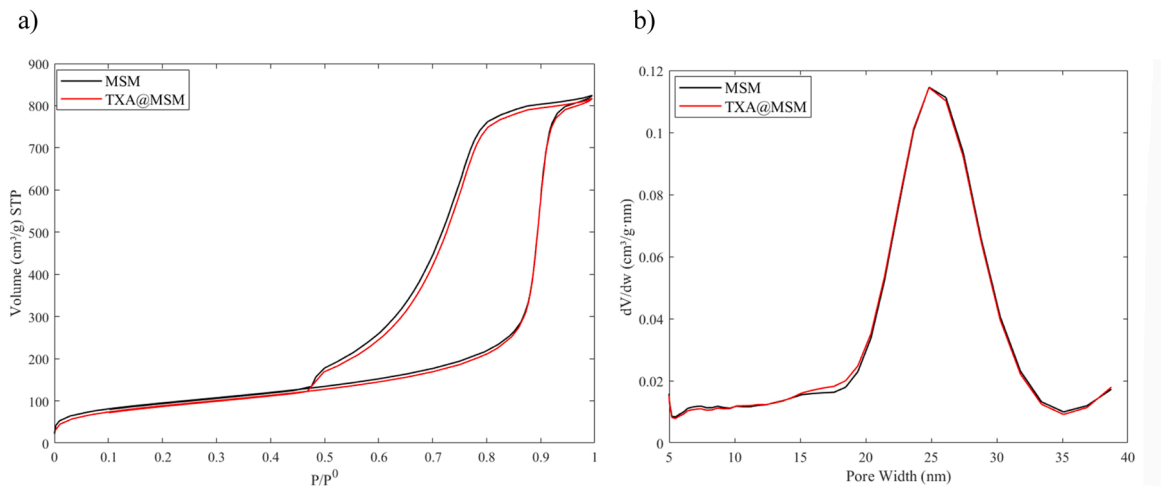

Fig. 2. (a) Nitrogen adsorption-desorption isotherms and (b) pore size distribution of the MSM and TXA@MSM.

Table 1
SSA_{BET} and pore volume of MSM and TXA@MSM.

	SSA_{BET} (m^2/g)	Pore volume (cm^3/g)
MSM	342	1.27
TXA@MSM	325	1.22

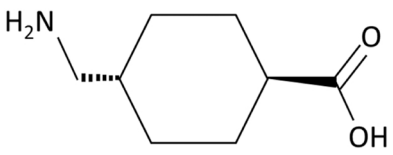

Scheme 1. : Chemical structure of tranexamic acid.

Fig. 3 compares the XRD patterns of MSM, TXA@MSM and pure TXA. The XRD pattern of pure TXA presents well-defined peaks of the crystalline phase [25]. On the other hand, the XRD patterns of MSM and TXA@MSM are typical of amorphous silica. The absence of the typical peaks of crystalline TXA in the TXA@MSM sample suggests that the molecules of the drug are dispersed inside the mesoporous carrier in non-crystalline form.

The FT-IR spectra of MSM and TXA@MSM are shown in Fig. 4. MSM exhibits the typical spectrum of amorphous silica with two main bands: a narrow band at 3740 cm^{-1} due to the isolated silanols and a broad absorption band at about 3500 cm^{-1} due to silanols interacting via H-bonding [26]. The spectrum of TXA@MSM shows a decrease in the intensity of the peak (3740 cm^{-1}) associated to the isolated silanols. In addition, a new broad absorption band appears in the 3500–2500 cm^{-1} range, which also shows two superimposed narrower bands at 2934 cm^{-1} and 2858 cm^{-1}, respectively. The decrease in the intensity of the peak ascribed to isolated silanols (3740 cm^{-1}) suggests the occurrence of H-bonding interactions between the isolated silanols and TXA molecules, which is also responsible for the new broad absorption below 3500 cm^{-1}. The narrower bands at 2934 cm^{-1} and 2858 cm^{-1} are attributed to the stretching vibrations of the -CH_2- groups of TXA [27]. Other bands ascribed to TXA can be observed at lower wavenumbers. In particular, an intense band appears between 1600 cm^{-1} and 1500 cm^{-1}, which can be attributed to the symmetric deformation mode of protonated amine groups -NH_3^+ [28,29]. A second intense band is observed at about 1400 cm^{-1}, which is ascribed to both the bending vibrations (wegging) of -CH_2- groups [27] and the symmetric stretching vibration of carboxylate -COO^- species [28,30]. The antisymmetric stretching vibration of the same COO^- groups, which is expected to appear in the spectrum above 1500 cm^{-1}, more likely contributes to the band observed between 1600 cm^{-1} and 1500 cm^{-1}. Moreover, two weaker bands can be observed at about 1630 cm^{-1} and 1450 cm^{-1}, which are ascribed to the bending modes (scissoring) of the amine and -CH_2- groups of TXA, respectively [27]. Residual molecular water adsorbed on the sample could also contribute to the absorption band at about 1630 cm^{-1}.

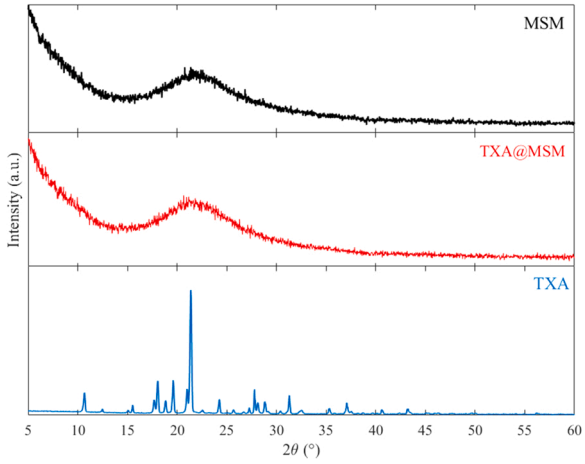

Fig. 3. XRD patterns of MSM, TXA@MSM and pure TXA.

The above discussed spectroscopic results suggest that TXA has been deposited on the silica surface mainly in the form of zwitterionic species [20,29].

3.2. Blood clotting time test

The in vitro hemostatic efficiency of MSM and TXA@MSM was evaluated by blood clotting time (BCT) test, a method which measures the time that blood needs to form a clot. As shown in Fig. 5, the clotting time was significantly shortened by MSM as well as by TXA@MSM when compared to control. In addition, the test showed that there was no difference in the clotting time between the two samples. This is due to the fact that TXA is an antifibrinolytic drug, so it exerts its hemostatic action not by inducing the formation of a clot, but preventing clot dissolution [19] in a longer time.

In conclusion, the results of the BCT test indicated that both samples exhibited good hemostatic performance, and that the presence of TXA on the surface of the material did not affect the ability of MSM in inducing the activation of the coagulation cascade.

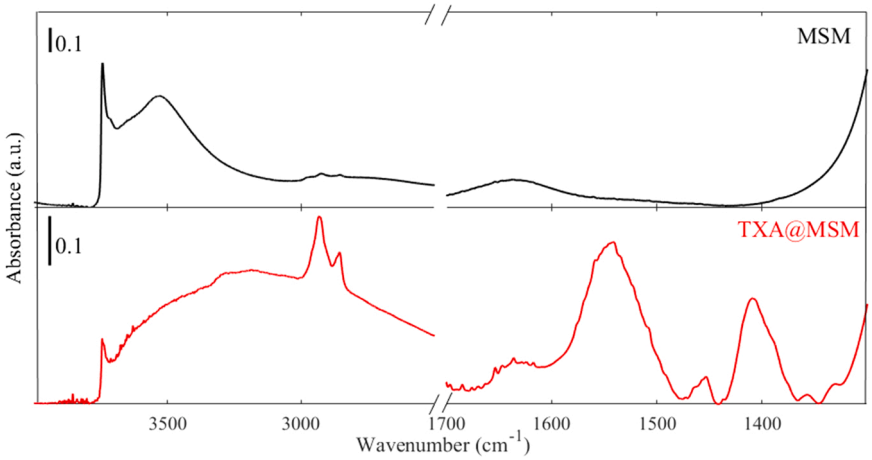

Fig. 4. FT-IR Spectra of MSM (black curve) and TXA@MSM (red curve).

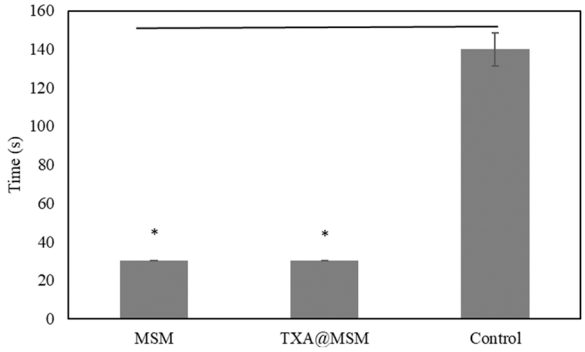

Fig. 5. BCT time for MSM, TXA@MSM and control. Data are represented as mean ± SD (n = 3). * Significant difference ($p < 0.05$) analyzed by one-way ANOVA.

3.3. Hemolysis assay

Besides its efficiency, a hemostatic material should not cause damage to blood components. It is known that silica based materials could cause damage to the membrane of red blood cells [31–33]. Therefore, a hemolysis assay was carried out to evaluate the hemolytic behavior of MSM. Fig. 6 reports the hemolysis ratio of MSM at two different concentrations (i.e., 100 and 500 μg/ml). The results of the test showed that no significant hemolytic activity was observed at the two concentrations. In conclusion, the hemolysis assay revealed that MSM showed a high hemocompatibility toward the red blood cells.

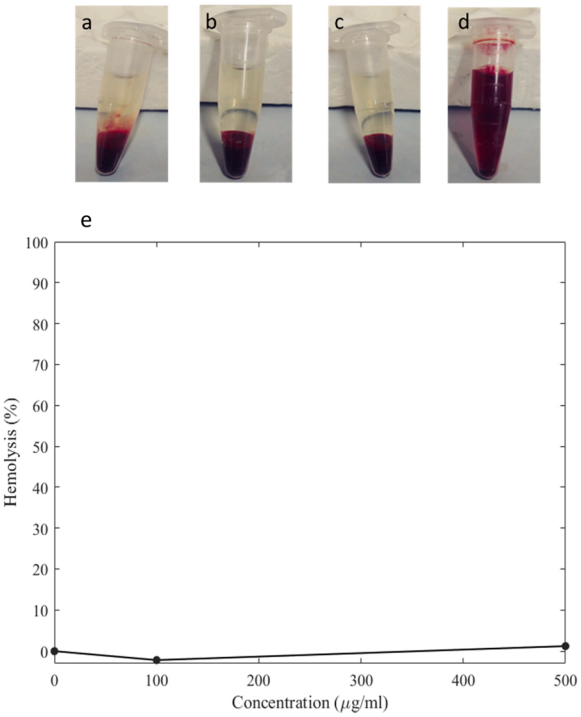

Fig. 6. Hemolysis assay on MSM. Photographs of hemolysis of red blood cells (a) negative control, (b) MSM-100 μg/ml, (c) MSM-500 μg/ml, (d) positive control and (e) percentage of hemolysis of red blood cells.

3.4. In vitro release of TXA

The preliminary in vitro release test aimed at verifying the possibility of a fast release of the drug from the microspheres. Fast release, in fact, is considered an important factor in bleeding control. Indeed, according to the CRASH-2 (Clinical Randomization of an Antifibrinolytic in Significant Hemorrhages-2) trial, early administration of TXA to control hemorrhages is fundamental in reducing the risk of death in bleeding trauma patients, without increasing the risk of developing thrombosis. The maximum efficiency can be obtained when TXA is administered within one hour of the traumatic event [34].

In order to evaluate the drug release from TXA@MSM, an FT-IR analysis (Fig. 7) was carried out on the powder recovered after the release test (60 min). The FTIR spectrum of TXA@MSM did not show any band related to TXA, so confirming its total release within an hour. The obtained result is crucial since, as mentioned earlier, the maximum efficacy is achieved when the administration of TXA occurs within the first hour.

In conclusion, the preliminary in vitro release test suggests that MSM could be a suitable carrier for the release of TXA as it is able to deliver it in a rapid manner, which is desirable for its use in the management of bleeding during first aid situations.

Beyond evaluating the release of TXA from the microspheres, it is important to assess if the drug can limit fibrinolysis or not. Generally, fibrinolysis is studied by monitoring the changes in turbidity during clot formation and its subsequent lysis [35,36] with a spectrophotometer. Unfortunately, this technique cannot be applied to the investigated system since the presence of silica microspheres affects turbidity so interfering with the analysis. In order to obtain some preliminary insight on this point, clot lysis was evaluated through a simple qualitative approach based on the observation of the flow of plasma inside an

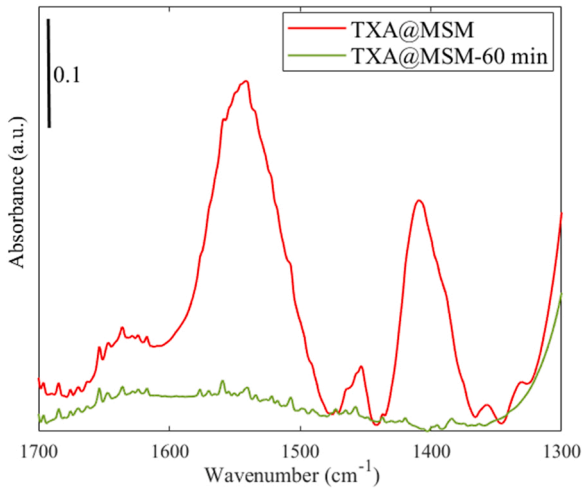

Fig. 7. FT-IR Spectra of TXA@MSM- before and after release test.

eppendorf tube. First, the clotting of plasma was induced; as a result, plasma stopped flowing through the walls of the tube when this was tilted. Then, a thrombolytic drug was added to induce the clot lysis of the plasma, which started flowing again. The extent of the clot lysis was estimated by observing the flow of the plasma after the addition of the thrombolytic drug to the clot. The results of the test showed that in the presence of TXA@MSM the flow was much slower with respect to the samples treated with pure TXA or MSM, suggesting that TXA@MSM can limit fibrinolysis. However, more accurate tests need to be implemented in order to confirm this behavior.

4. Conclusions

A novel hemostatic material to be used for the control of hemorrhages in emergency has been proposed for the first time. The obtained material combines the hemostatic ability of mesoporous silica with the antifibrinolytic activity of tranexamic acid. MSM (with particle sizes ranging from 1 to 5 μm and an average pore diameter of 25 nm) were synthesized, characterized, and loaded with TXA (with a final content of 4.7%w/w) through an incipient wetness impregnation technique by using water as a solvent. The XRD analysis revealed that TXA was distributed inside the carrier in non-crystalline form. The FT-IR analysis showed that TXA molecules were dispersed on the mesopore silica surface in their zwitterionic form. BCT tests performed on both the unimpregnated and impregnated MSM indicated that both systems were able to activate the coagulation cascade. A hemolysis assay was performed to evaluate the hemolytic activity of MSM, and the result indicated that the material was blood compatible. The preliminary in *vitro* release of TXA showed that the material was able to deliver TXA to the release medium within one hour, as suggested from the CRASH-2 trial in order to achieve maximum efficiency in the hemorrhage control. Furthermore, a preliminary clot lysis evaluation indicated that impregnated MSM can limit fibrinolysis.

In conclusion, the aim of this study was to combine tranexamic acid, a clinically used antifibrinolytic agent, and mesoporous silica microspheres (MSM), to develop a novel material with intrinsic hemostatic properties. The preliminary results suggest that the proposed system is promising for the future development of new hemostats suitable for bleeding control in emergency situations. The present work can open the way to future investigations of the in vitro and in vivo behavior of the proposed system.

Funding

This research did not receive any specific grant from funding agencies in the public, commercial, or not-for-profit sectors.

Declaration of Competing Interest

The authors declare that they have no known competing financial interests or personal relationships that could have appeared to influence the work reported in this paper.

Data Availability

Data will be made available on request.

Appendix A. Supporting information

Supplementary data associated with this article can be found in the online version at doi:10.1016/j.mtcomm.2022.105198.

References

[1] D.R. Spahn, B. Bouillon, V. Cerny, J. Duranteau, D. Filipescu, B.J. Hunt, R. Komadina, M. Maegele, G. Nardi, L. Riddez, C.-M. Samama, J.-L. Vincent, R. Rossaint, The European guideline on management of major bleeding and coagulopathy following trauma: fifth edition, Crit. Care 23 (2019) 98, https://doi.org/10.1186/s13054-019-2347-3.

[2] D.S. Kauvar, R. Lefering, C.E. Wade, Impact of hemorrhage on trauma outcome: an overview of epidemiology, clinical presentations, and therapeutic considerations, J. Trauma Inj. Infect. Crit. Care 60 (2006) S3–S11, https://doi.org/10.1097/01.ta.0000199961.02677.19.

[3] J.A. Chambers, K. Seastedt, R. Krell, E. Caterson, M. Levy, N. Turner, "Stop the bleed": A U.S. military installation's model for implementation of a rapid hemorrhage control program, Mil. Med 184 (2019) 67–71, https://doi.org/10.1093/milmed/usy185.

[4] M.A. Schreiber, D.J. Neveleff, Achieving hemostasis with topical hemostats: Making clinically and economically appropriate decisions in the surgical and trauma settings, AORN J. 94 (2011) S1–S20, https://doi.org/10.1016/j.aorn.2011.09.018.

[5] R. Liu, L. Dai, C. Si, Z. Zeng, Antibacterial and hemostatic hydrogel via nanocomposite from cellulose nanofibers, Carbohydr. Polym. 195 (2018) 63–70, https://doi.org/10.1016/j.carbpol.2018.04.085.

[6] S. Pourshahrestani, E. Zeimaran, I. Djordjevic, N.A. Kadri, M.R. Towler, Inorganic hemostats: the state-of-the-art and recent advances, Mater. Sci. Eng. C. 58 (2016) 1255–1268, https://doi.org/10.1016/j.msec.2015.09.008.

[7] L. Huang, G.L. Liu, A.D. Kaye, H. Liu, Advances in topical hemostatic agent therapies: a comprehensive update, Adv. Ther. 37 (2020) 4132–4148, https://doi.org/10.1007/s12325-020-01467-y.

[8] J.K. Wright, J. Kalns, E.A. Wolf, F. Traweek, S. Schwarz, C.K. Loeffler, W. Snyder, L. D. Yantis, J. Eggers, Thermal injury resulting from application of a granular mineral hemostatic agent, J. Trauma Inj. Infect. Crit. Care 57 (2004) 224–230, https://doi.org/10.1097/01.TA.0000105916.30158.06.

[9] S.E. Baker, A.M. Sawvel, J. Fan, Q. Shi, N. Strandwitz, G.D. Stucky, Blood clot initiation by mesocellular foams: dependence on nanopore size and enzyme immobilization, Langmuir 24 (2008) 14254–14260, https://doi.org/10.1021/la802804z.

[10] C. Dai, Y. Yuan, C. Liu, J. Wei, H. Hong, X. Li, X. Pan, Degradable, antibacterial silver exchanged mesoporous silica spheres for hemorrhage control, Biomaterials 30 (2009) 5364–5375, https://doi.org/10.1016/j.biomaterials.2009.06.052.

[11] X. Wu, J. Wei, X. Lu, Y. Lv, F. Chen, Y. Zhang, C. Liu, Chemical characteristics and hemostatic performances of ordered mesoporous calcium-doped silica xerogels, Biomed. Mater. 5 (2010), https://doi.org/10.1088/1748-6041/5/3/035006.

[12] C. Dai, C. Liu, J. Wei, H. Hong, Q. Zhao, Molecular imprinted macroporous chitosan coated mesoporous silica xerogels for hemorrhage control, Biomaterials 31 (2010) 7620–7630, https://doi.org/10.1016/j.biomaterials.2010.06.049.

[13] Y. Li, A.M. Sawvel, Y.S. Jun, S. Nownes, M. Ni, D. Kudela, G.D. Stucky, D. Zink, Cytotoxicity and potency of mesocellular foam-26 in comparison to layered clays used as hemostatic agents, Toxicol. Res. (Camb.). 2 (2013) 136–144, https://doi.org/10.1039/c2tx20065a.

[14] Z. Chen, F. Li, C. Liu, J. Guan, X. Hu, G. Du, X. Yao, J. Wu, F. Tian, Blood clot initiation by mesoporous silica nanoparticles: dependence on pore size or particle size? J. Mater. Chem. B 4 (2016) 7146–7154, https://doi.org/10.1039/c6tb01946c.

[15] H. Hong, C. Wang, Y. Yuan, X. Qu, J. Wei, Z. Lin, H. Zhou, C. Liu, Novel porous silica granules for instant hemostasis, RSC Adv. 6 (2016) 78930–78935, https://doi.org/10.1039/c6ra13999j.

[16] D. Li, W. Nie, L. Chen, Y. Miao, X. Zhang, F. Chen, B. Yu, R. Ao, B. Yu, C. He, Fabrication of curcumin-loaded mesoporous silica incorporated polyvinyl pyrrolidone nanofibers for rapid hemostasis and antibacterial treatment, RSC Adv. 7 (2017) 7973–7982, https://doi.org/10.1039/c6ra27319j.

[17] C. Wang, H. Zhou, H. Niu, X. Ma, Y. Yuan, H. Hong, C. Liu, Tannic acid-loaded mesoporous silica for rapid hemostasis and antibacterial activity, Biomater. Sci. 6 (2018) 3318–3331, https://doi.org/10.1039/c8bm00837j.

[18] S. Pourshahrestani, N.A. Kadri, E. Zeimaran, M.R. Towler, Well-ordered mesoporous silica and bioactive glasses: promise for improved hemostasis, Biomater. Sci. 7 (2019) 31–50, https://doi.org/10.1039/c8bm01041b.
[19] P.L. McCormack, Tranexamic acid: a review of its use in the treatment of hyperfibrinolysis, Drugs 72 (2012) 585–617, https://doi.org/10.2165/11209070-000000000-00000.
[20] S. Sarda, F. Errassifi, O. Marsan, A. Geffre, C. Trumel, C. Drouet, Adsorption of tranexamic acid on hydroxyapatite: Toward the development of biomaterials with local hemostatic activity, Mater. Sci. Eng. C 66 (2016) 1–7, https://doi.org/10.1016/j.msec.2016.04.032.
[21] K. Ker, D. Beecher, I. Roberts, Topical application of tranexamic acid for the reduction of bleeding, Cochrane Database Syst. Rev. 2013 (2013), https://doi.org/10.1002/14651858.CD010562.pub2.
[22] Q.K. Zhong, Z.Y. Wu, Y.Q. Qin, Z. Hu, S.D. Li, Z.M. Yang, P.W. Li, Preparation and properties of carboxymethyl chitosan/alginate/tranexamic acid composite films, Membranes 9 (2019), https://doi.org/10.3390/membranes9010011.
[23] L. Wang, T. Qi, Y. Zhang, J. Chu, Morphosynthesis route to large-pore SBA-15 microspheres, Microporous Mesoporous Mater. 91 (2006) 156–160, https://doi.org/10.1016/j.micromeso.2005.11.042.
[24] M. Thommes, K. Kaneko, A. Neimark, J. Olivier, F. Rodriguez-Reinoso, J. Rouquerol, K. Sing, Physisorption of gases, with special reference to the evaluation of surface area and pore size distribution (IUPAC Technical Report, Pure Appl. Chem. 87 (2015), https://doi.org/10.1515/pac-2014-1117.
[25] S.S. Bhattacharya, S. Banerjee, P. Chowdhury, A. Ghosh, R.R. Hegde, R. Mondal, Tranexamic acid loaded gellan gum-based polymeric microbeads for controlled release: In vitro and in vivo assessment, Colloids Surf. B Biointerfaces 112 (2013) 483–491, https://doi.org/10.1016/j.colsurfb.2013.07.054.
[26] P.U.A. Rimola, D. Costa, M. Sodupe, J.-F. Lambert, Silica Surface Features And Their Role In The Adsorption Of Biomolecules: Computational Modeling And Experiments, Chem. Rev. 113 (2013) 4216–4313, https://doi.org/10.1021/cr3003054.
[27] S. Muthu, A. Prabhakaran, Vibrational spectroscopic study and NBO analysis on tranexamic acid using DFT method, Spectrochim. Acta - Part A Mol. Biomol. Spectrosc. 129 (2014) 184–192, https://doi.org/10.1016/j.saa.2014.03.050.
[28] G. Socrates, Infrared and Raman characteristic group frequencies, Tables Charts (2001).
[29] T. Shaikh, A. Nafady, F.N. Talpur, M.H. Sirajuddin, M.R. Agheem, S.T.H. Shah, R. A. Sherazi, S. Soomro, Siddiqui, Tranexamic acid derived gold nanoparticles modified glassy carbon electrode as sensitive sensor for determination of nalbuphine, Sens. Actuators B Chem. 211 (2015) 359–369, https://doi.org/10.1016/j.snb.2015.01.096.
[30] M. Meng, L. Stievano, J.F. Lambert, Adsorption and thermal condensation mechanisms of amino acids on oxide supports. 1, Glycine silica, Langmuir 20 (2004) 914–923, https://doi.org/10.1021/la035336b.
[31] A. Yildirim, E. Ozgur, M. Bayindir, Impact of mesoporous silica nanoparticle surface functionality on hemolytic activity, thrombogenicity and non-specific protein adsorption, J. Mater. Chem. B 1 (2013) 1909–1920, https://doi.org/10.1039/c3tb20139b.
[32] A.J. Paula, D.S.T. Martinez, R.T.A. Júnior, A.G.S. Filho, O.L. Alves, Suppression of the hemolytic effect of mesoporous silica nanoparticles after protein corona interaction: Independence of the surface microchemical environment, J. Braz. Chem. Soc. 23 (2012) 1807–1814, https://doi.org/10.1590/S0103-50532012005000048.
[33] J. Shi, Y. Hedberg, M. Lundin, I. Odnevall Wallinder, H.L. Karlsson, L. Möller, Hemolytic properties of synthetic nano- and porous silica particles: The effect of surface properties and the protection by the plasma corona, Acta Biomater. 8 (2012) 3478–3490, https://doi.org/10.1016/j.actbio.2012.04.024.
[34] F. Olldashi, M. Kerçi, T. Zhurda, K. Ruçi, A. Banushi, M.S. Traverso, J. Jiménez, J. Balbi, C. Dellera, S. Svampa, G. Quintana, G. Piñero, J. Teves, I. Seppelt, D. Mountain, J. Hunter, Z. Balogh, M. Zaman, P. Druwé, R. Rutsaert, G. Mazairac, F. Pascal, Z. Yvette, D. Chancellin, P. Okwen, J. Djokam-Liapoe, E. Jangwa, L. Mbuagbaw, N. Fointama, N. Pascal, F. Baillie, J.Y. Jiang, G.Y. Gao, Y.H. Bao, C. Morales, J. Sierra, S. Naranjo, C. Correa, C. Gómez, J. Herrera, L. Caicedo, A. Rojas, H. Pastas, H. Miranda, A. Constaín, M. Perdomo, D. Muñoz, Á. Duarte, E. Vásquez, C. Ortiz, B. Ayala, H. Delgado, G. Benavides, L. Rosero, J. Mejía-Mantilla, A. Varela, M. Calle, J. Castillo, A. García, J. Ciro, C. Villa, R. Panesso, L. Flórez, A. Gallego, F. Puentes-Manosalva, L. Medina, K. Márquez, A.R. Romero, R. Hernández, J. Martínez, W. Gualteros, Z. Urbina, J. Velandia, F. Benítez, A. Trochez, A. Villarreal, P. Pabón, H. López, L. Quintero, A. Rubiano, J. Tamayo, M. Piñera, Z. Navarro, D. Rondón, B. Bujan, L. Palacios, D. Martínez, Y. Hernández, Y. Fernández, E. Casola, R. Delgado, C. Herrera, M. Arbolaéz, M. Domínguez, M. Iraola, O. Rojas, A. Enseñat, I. Pastrana, D. Rodríguez, S.Á. De La Campa, T. Fortún, M. Larrea, L. Aragón, A. Madrazo, P. Svoboda, M. Izurieta, A. Daccach, M. Altamirano, A. Ortega, B. Cárdenas, L. González, M. Ochoa, F. Ortega, F. Quichimbo, J. Guiñanzaca, I. Zavala, S. Segura, J. Jerez, D. Acosta, F. Yánez, R. Camacho, H. Khamis, H. Shafei, A. Kheidr, H. Nasr, M. Mosaad, S. Rizk, H. El Sayed, T. Moati, E. Hokkam, M. Amin, H. Lowis, M. Fawzy, N. Bedir, M. Aldars, V. Rodríguez, J. Tobar, J. Alvarenga, B. Shalamberidze, E. Demuria, N. Rtveliashvili, G. Chutkerashvili, D. Dotiashvili, T. Gogichaishvili, G. Ingorokva, D. Kazaishvili, B. Melikidze, N. Iashvili, G. Tomadze, M. Chkhikvadze, L. Khurtsidze, Z. Lomidze, D. Dzagania, N. Kvachadze, G. Gotsadze, V. Kaloiani, N. Kajaia, J. Dakubo, S. Naaeder, P. Sowah, A. Yusuf, A. Ishak, P. Selasi-Sefenu, B. Sibiri, S. Sarpong-Peprah, T. Boro, K. Bopaiah, K. Shetty, R. Subbiah, L. Mulla, A. Doshi, Y. Dewan, S. Grewal, P. Tripathy, J. Mathew, B. Gupta, A. Lal, M. Choudhury, S. Gupta, S. Gupta, A. Chug, V. Pamidimukkala, P. Jagannath, M. Maharaj, R. Vommi, N. Gudipati, W.H. Chhang, P. Patel, N. Suthar, D. Banker, J. Patel, S. Dharap, R. Kamble, S. Patkar, S. Lohiya, R. Saraf, D. Kumar, S. Parihar, R. Gupta, R. Mangual, D. Kooper, C. Mohapatra, S. David, W. Rajaleelan, A. Pangi, V. Saraf, S. Chikareddy, S. Mankar, A. Golhar, R. Sakhare, N. Wagh, D. Hazarika, P. Chaudhuri, P. Ketan, G. Purohit, Y. Purohit, M. Pandya, R. Gupta, S. Kiran, S. Walia, S. Goyal, S. Goyal, S. Goyal, A. Attri, R. Sharma, A. Oberai, M. Oberai, S. Oberoi, G.K. Tripathi, V. Peettakkandy, P. Karuthillath, P. Vadakammuriyil, J. Pol, S. Pol, M. Saste, S. Raul, S. Tiwari, N. Nelly, M. Chidambaram, V. Kollengode, S. Thampan, S. Rajan, S. Rajan, S. Raju, R. Sharma, S.V. Babu, C. Sumathi, P. Chatterjee, A. Agarwal, H. Magar, M. Magar, M. Singh, D. Gupta, K. Haloi, V. Sagdeo, P. Giri, N. Verma, R. Jariwala, A. Goti, A. Prabhu-Gaonkar, S. Utagi, M. Joshi, R. Agrawal, G. Sharma, G. Saini, V. Tewari, Y. Yadav, V. Parihar, N. Venkataramana, S. Rao, N. Reddy, S.G. Chander, V. Hathila, V. Das, K. Agaja, A. Purohit, A. Lahari, R. Bhagchandani, B. Vidyasagar, P.K. Sachan, T. Das, S. Vyas, S. Bhattacharjee, P. Sancheti, T. Manoj, M. Moideen, K. Pansey, V. P. Chandrasekaran, K. Saikia, H. Tata, S. Vhora, A. Shah, G. Rangad, S. Rajasekaran, S.T. Shankarlal, S. Devadoss, M. Saleem, H. Pillay, Z. Hazarika, P. Deshmukh, S.P. Murugappan, A. Jaiswal, D. Vangani, P. Modha, C. Chonzik, M. Praveen, V. Sethurayar, S. Ipe, N. Shetty, V. Jain, K. Shah, M. Dwikoryanto, N. Golden, K. Atmadjaya, K. Wiargitha, K. Sudiasa, G. Suwedagatha, F. Bal'afif, V. Budipramana, A. Lemuel, S. Chandra, F. Ama, E. Sherafatkazemzadeh, E. Moradi, A. Sheikhi, A. Ziaee, A. Fanaei, E. Hajinasrollah, A. Amini, B. Mohammad, N. Hadi, G. Perone, E. De Peri, A. Volpi, J. Johnson, M. Abe, V. Mutiso, B. Okanga, D. Ojuka, B. Abdullah, H. Rahman, Y. Noh, S. Jamaluddin, H. Dawal, A. Roslani, C.W. Law, P. Devashanti, Y. Wahab, S. Velaiutham, R. Dato, J. Loría, E. Montes, E. Gómez, V. Cazales, P. Bautista, R. Bautista, D. Ahumada, E. Hernández, G. Velásquez, P. Ortega, G. Lira, F. Estrada, J. Martínez, J. Martínez, O. Olaomi, Y. Abubakar, K. Apollo, O. Badejo, O. Ihekire, J. Casasola, P. Iribhogbe, O. Oludiran, E. Obeta, C. Okojie, E.U. Agbon, E. Komolafe, P. Olaleye, T. Uzochukwu, U. Onakpoya, A. Dongo, O. Uhunmwagho, E. Eighemerio, E. Morgan, L. Thanni, A. Afolabi, T. Akinola, A. Ademola, O. Akute, L. Khalid, L. Abubakar, M. Aminu, M. Ogirima, A. Attansey, D. Michael, O. Aremu, O. Olugbenga, U. Ukpong, Y. Salman, N. Obianyo, C. Ani, R. Ezeadawi, O. Kehinde, A. Olaide, A. Jogo, T. Bitto, S. Anyanwu, O. Mbonu, M. Oludara, M. Somoye, B. Shehu, N. Ismail, A. Katchy, R. Ndoma-Egba, N. Grace-Inah, Z. Songden, A. Abdulraheem, A. Otu, T. Nottidge, D. Inyang, D. Idiapho, H. Giebel, R. Hassan, A. Adisa, A. Akinkuolie, K. Okam, A. Musa, I. Falope, J. Eze, J. Caballero, W. Azabache, O. Salirrosas, A. Soto, E. Torres, G. Ramírez, M. Pérez, C. Malca, J. Velez, R. Yepez, H. Yupanqui, P. Lagos, D. Rodriguez, J. Flores, A. Moya, A. Barrionuevo, M. Gonzales-Portillo, E. Nunez, A. Eldawlatly, M. Al Naami, B. Delvi, W. Alyafi, B. Djurovic, I. Ng, A. Yaghi, A. Laincz, S. Trenkler, J. Valky, M. Modiba, P. Legodi, T. Rangaka, L. Wallis, Á. Muñoz, A. Serrano, M. Misis, M. Rubi, V. De La Torre, R. Ellawala, S. Wijeratna, L. Gunaratna, C. Wijayanayaka, K. Nungu, B. Haonga, G. Mtapa, S. Yutthakasemsunt, W. Kittiwattanagul, P. Piyavechvirat, T. Impool, S. Thummaraj, R. Salaeh, S. Tangchitvittaya, K. Wattanakrai, C. Soonthornthum, T. Jiravongbunrod, S. Meephant, P. Subsompon, P. Pensuwan, W. Chamnongwit, Z. Jerbi, A. Cherif, M. Nash, T. Harris, J. Banerjee, R. Freij, J. Kendall, S. Moore, W. Townend, R. Cottingham, D. Becker, S. Lloyd, P. Burdett-Smith, K. Mirza, A. Webster, S. Brady, A. Grocutt, J. Thurston, F. Lecky, S. Goodacre, Y. Mulla, D. Sakala, C. Chengo, Effects of tranexamic acid on death, vascular occlusive events, and blood transfusion in trauma patients with significant haemorrhage (CRASH-2): A randomised, placebo-controlled trial, Lancet 376 (2010) 23–32, https://doi.org/10.1016/S0140-6736(10)60835-5.
[35] J.C. Fredenburgh, M.E. Nesheim, Lys-plasminogen is a significant intermediate in the activation of Glu-plasminogen during fibrinolysis in vitro, J. Biol. Chem. 267 (1992) 26150–26156, https://doi.org/10.1016/S0021-9258(18)35729-6.
[36] T. Lisman, P.G. de Groot, J.C.M. Meijers, F.R. Rosendaal, Reduced plasma fibrinolytic potential is a risk factor for venous thrombosis, Blood 105 (2005) 1102–1105, https://doi.org/10.1182/blood-2004-08-3253.